NATIONAL ADVISORY COMMITTEE FOR AERONAUTICS

TECHNICAL NOTE 2976

A STUDY OF THE STABILITY OF THE INCOMPRESSIBLE LAMINAR BOUNDARY LAYER ON INFINITE WEDGES

By Neal Tetervin

Langley Aeronautical Laboratory
Langley Field, Va.

Washington
August 1953

NATIONAL ADVISORY COMMITTEE FOR AERONAUT

TECHNICAL NOTE 2976

A STUDY OF THE STABILITY OF THE INCOMPRESSIBLE LAMINAR BOUNDARY LAYER ON INFINITE WEDGES

By Neal Tetervin

SUMMARY

The flow over infinite wedges is investigated theoretically to test a conclusion previously reached by the use of Schlichting's approximate method for the calculation of the laminar boundary layer; namely, that in a region of falling pressure a thick velocity profile can be more stable than a thin profile although the velocity at the edge of the boundary layer and the pressure gradient are the same for both profiles. By the use of the velocity profiles obtained by Hartree from a numerical solution of the boundary-layer equations for wedge flows and by the use of Lin's rapid method for the calculation of the critical Reynolds number of a velocity profile, the result is obtained that a thick velocity profile on one wedge can be more stable than a thinner profile on a wedge of different angle although the velocity outside the boundary layer and the pressure gradient are the same for both profiles. This result agrees with, and hence confirms, a conclusion reached by the use of Schlichting's approximate method.

The investigation also leads to the inference that the calculated effects of a change in boundary-layer thickness on the stability and on the local roughness Reynolds number should be essentially unchanged by replacing the Schlichting single-parameter family of velocity profiles by the Hartree single-parameter family of velocity profiles.

INTRODUCTION

Experimental investigations have shown that large extents of laminar flow can be obtained on airfoils by making the pressure decrease along the surface in the direction of flow, by drawing part of the boundary layer into the airfoil interior either through a porous airfoil surface or through slots cut into the surface, or by a combination of these methods. The experiments, however, make it clear that, to avoid early transition to turbulent flow, the surface must be free of noticeable roughness particles and other departures from smoothness.

The indications are that the disturbing effect of a roughness particle can be decreased by an increase in the thickness of the boundary layer. An increase in boundary-layer thickness, however, increases the boundary-layer Reynolds number and, if the shape of the velocity profile is unchanged, decreases the ratio of the local critical Reynolds number to the local boundary-layer Reynolds number. The assumption is made that the ratio of the local critical Reynolds number (a function of the shape of the velocity profile only) to the local boundary-layer Reynolds number is a measure of the stability; the stability decreases as this ratio decreases. For a fixed velocity-profile shape, the stability of the boundary layer thus decreases as the thickness increases.

The shape of the velocity profile and the thickness of the boundary layer at a point on a porous or nonporous surface with an arbitrary pressure distribution can be calculated approximately by the Schlichting method (ref. 1). This method states that on an impervious surface the shape of the velocity profile is determined by the local effective pressure gradient; this gradient is directly proportional to the product of the actual pressure gradient and the square of the boundary-layer thickness. It is apparent, therefore, that in a region of falling pressure the Schlichting method predicts that an increase in boundary-layer thickness increases the effective pressure gradient and thus results in a more convex velocity profile. Because the increase in convexity is known to imply an increase in the critical boundary-layer Reynolds number, it would appear that an increase in boundary-layer thickness could increase the local critical Reynolds number more than the local boundary-layer Reynolds number.

The computations of reference 2, which were made to investigate this possibility, led to the result that where the pressure decreases along an impermeable surface an increase in boundary-layer thickness at a point can, because of the resulting increase in effective pressure gradient, change the velocity-profile shape enough to increase the ratio of the local critical Reynolds number to the local boundary-layer Reynolds number, and hence increase the stability.

Because the results of reference 2 follow from the Schlichting method, an approximate method, it is desirable to examine the available exact solutions of the boundary-layer equations to determine whether solutions exist that can be used to test the results of reference 2. The exact solutions of the boundary-layer equations, however, are few, and the only solutions that were found suitable for use as a test were the solutions for the flow over infinite wedges.

The method by which the wedge flows are used to test the results of reference 2 makes use of the fact that the Schlichting method states that the shape of a velocity profile is completely determined by the local value of the nondimensional pressure gradient. The previous history of

the boundary layer enters only indirectly. Therefore, the result of reference 2 can also be stated in a different manner. Thus, consider two incompressible flows with the same kinematic viscosity and let one flow contain a point such that the velocity outside the boundary layer and the pressure gradient along the surface are equal, respectively, to the velocity outside the boundary layer and to the pressure gradient at a point in another flow. Then, if the boundary-layer thickness is not the same at the two points, the thicker boundary-layer velocity profile can be the more stable one.

In the present investigation a confirmation of this conclusion is sought by examining the exact solutions of the boundary-layer equations for wedge flows, the special set of flows in which the velocity outside the boundary layer varies as the distance from the stagnation point raised to a power. Numerical solutions of the boundary-layer equations for these flows have been given by Hartree (ref. 3).

Whether the results of reference 2 are always valid is not tested in the present work because the wedge flows satisfy a basic assumption of the Schlichting method; namely, that the velocity profile is a single-valued function of the local effective pressure gradient. Therefore, if in certain cases the rate of change of the velocity profile along the surface would make inaccurate the assumption that the velocity-profile shape depends only on the local effective pressure gradient, significant errors might be introduced into the results of reference 2. These errors cannot be uncovered by the use of the wedge flows. The wedge flows consequently provide only a partial test of the results of reference 2.

In the present investigation information is also obtained concerning the effect on the conclusions of reference 2 of replacing the Schlichting single-parameter family of velocity profiles by the Hartree single-parameter family of velocity profiles. This portion of the investigation is desirable because the critical Reynolds number is sensitive to the shape of the velocity profile. An accurate numerical calculation, based on Lin's rapid method, is made of the critical Reynolds numbers of all the Hartree velocity profiles. The present investigation is restricted to the case of no flow through the surface.

SYMBOLS

$\bar{a}$ constant, equal numerically to velocity at $\bar{x} = 1$

$$a = \frac{\bar{a}\bar{c}^{\frac{\beta}{2-\beta}}}{\bar{U}_o}$$

C_o, C_1, C_2 coefficients in expression for g

$\bar{c}$ reference length

F function of Y

$$g = \frac{\bar{\theta}}{\bar{\delta}_1} = C_o + C_1 K + C_2 K^2$$

$\bar{h}$ height of roughness particle

$$k = \frac{\bar{\theta}^2}{\bar{\nu}} \frac{d\bar{U}}{d\bar{x}} = \frac{R_\theta{}^2}{R_c} \frac{1}{U^2} \frac{dU}{dx}$$

$$k_1 = - \frac{v_w}{U} R_\theta$$

K Schlichting velocity-profile shape parameter

$\bar{u}$ velocity in direction of $\bar{x}$

$\bar{U}$ velocity at outer edge of boundary layer

$$U = \frac{\bar{U}}{\bar{U}_o}$$

$\bar{U}_o$ reference velocity (velocity at distance $\bar{c}$ from apex of reference wedge)

$\bar{u}_c$ velocity of disturbance in boundary layer

$\bar{u}_h$ velocity at $\bar{y} = \bar{h}$ with roughness particle absent

R_c reference Reynolds number, $\bar{U}_o \bar{c} / \bar{\nu}$

$$R_\theta = \frac{\bar{U}\bar{\theta}}{\bar{\nu}}$$

R_{θ_c} critical Reynolds number, value of R_θ at which a small disturbance is neither damped nor amplified

R_h roughness Reynolds number, $\bar{u}_h\bar{h}/\bar{\nu}$

$v_w = \frac{\bar{v}_w}{\bar{U}_o}$

$\bar{v}_w$ velocity through surface, positive outward

$\bar{x}$ distance along surface, measured from stagnation point

$x = \frac{\bar{x}}{\bar{c}}$

$\bar{y}$ distance normal to surface, positive outward

Y nondimensional distance from surface, $\frac{\bar{y}}{\sqrt{2 - \beta}}\sqrt{\frac{\bar{U}}{\bar{\nu}\bar{x}}}$

β parameter

β_o value of parameter β for reference wedge

$\bar{\delta}^*$ displacement thickness, $\int_0^\infty \left(1 - \frac{\bar{u}}{\bar{U}}\right)d\bar{y}$

$\bar{\delta}_1$ a measure of boundary-layer thickness

$\bar{\theta}$ momentum thickness of boundary layer, $\int_0^\infty \frac{\bar{u}}{\bar{U}}\left(1 - \frac{\bar{u}}{\bar{U}}\right)d\bar{y}$

ϕ function of Y

$\bar{\psi}$ stream function

$\bar{\nu}$ kinematic viscosity

α angle between walls of wedge, radians

Subscript:

w at surface

Primes denote differentiation with respect to Y; barred quantities are dimensional.

ANALYSIS

Comparison of Wedge Flows

The first portion of the present investigation is restricted to those incompressible laminar flows for which the velocity outside the boundary layer is related to the distance from the stagnation point by the equation

$$\bar{U} = \bar{a}\bar{x}^{\frac{\beta}{2-\beta}} \tag{1}$$

which is obtained from reference 4, pages 139 to 142, but put in the notation of the present paper. There is no flow through the surface in the present analysis. For $\beta \geqq 0$ the flow is that over the inner or outer face of an infinite wedge with an angle 2α between the walls (fig. 1(a)). The relation between α and the parameter β is

$$\alpha = \frac{\pi\beta}{2}$$

This relation also occurs, in a different notation, on page 3 of reference 5. Only values of β less than 2 have physical significance. For $\beta < 0$ (fig. 1(b)) the flow begins at a value of x greater than zero with a boundary-layer-profile shape that depends on the parameter β.

In the wedge flow defined by equation (1) the velocity $\bar{U}$ and the velocity derivative $\frac{d\bar{U}}{d\bar{x}}$ are single-valued functions of $\bar{x}$. Consequently, two points with equal $\bar{U}$ and $\frac{d\bar{U}}{d\bar{x}}$ cannot be found on the same wedge. If, however, two wedges with different angles are considered, and if the velocity at a point on one wedge is properly related to the velocity at a point on the other wedge, then two points can be found, one on each wedge, with the same $\bar{U}$ and $\frac{d\bar{U}}{d\bar{x}}$.

In order to find the relation between the wedge angles and the two points, one on each wedge, that have equal $\bar{U}$ and $\frac{d\bar{U}}{d\bar{x}}$, let

$$U_{x_2} = U_{x_1} \tag{2}$$

and

$$\left(\frac{dU}{dx}\right)_{x_2} = \left(\frac{dU}{dx}\right)_{x_1} \tag{3}$$

where U_{x_2} and $\left(\frac{dU}{dx}\right)_{x_2}$ are the nondimensional velocity and velocity gradient, respectively, in one flow at $x = x_2$, and U_{x_1} and $\left(\frac{dU}{dx}\right)_{x_1}$ are the same quantities in the other flow at $x = x_1$. The reference velocity $\bar{U}_o$ and the reference length $\bar{c}$ are the same in both flows. The reference velocity $\bar{U}_o$ can be chosen as the velocity at a distance $\bar{c}$ from the apex of a fixed reference wedge of included angle $\pi\beta_o$. The quantity $\bar{a}$ (eq. (1)) has the value $\bar{a}_o$ for the reference flow and it is found from $\bar{U}_o$, $\bar{c}$, and β_o by the use of equation (1):

$$\bar{a}_o = \frac{\bar{U}_o}{\frac{\beta_o}{\bar{c}^{2-\beta_o}}}$$

The quantities $\bar{U}_o$, $\bar{c}$, and $\bar{\beta}_o$ are arbitrary but when once chosen are fixed.

For $\beta = \beta_1$, equation (1) becomes

$$\bar{U}_{\bar{x}_1} = \bar{a}_1 \bar{x}_1^{\frac{\beta_1}{2-\beta_1}}$$

or

$$U_{x_1} = a_1 x_1^{\frac{\beta_1}{2-\beta_1}} \tag{4}$$

where

$$a_1 = \frac{\bar{U}_{\bar{x}_1=\bar{c}}}{\bar{U}_o} = \frac{\bar{a}_1 \bar{c}^{\frac{\beta_1}{2-\beta_1}}}{\bar{U}_o}$$

For $\beta = \beta_2$, equation (1) becomes

$$U_{x_2} = a_2 x_2^{\frac{\beta_2}{2-\beta_2}} \tag{5}$$

where

$$a_2 = \frac{\bar{U}_{\bar{x}_2=\bar{c}}}{\bar{U}_o} = \frac{\bar{a}_2 \bar{c}^{\frac{\beta_2}{2-\beta_2}}}{\bar{U}_o}$$

The condition that $\bar{U}$ at $\bar{x}_1$ be equal to $\bar{U}$ at $\bar{x}_2$ (eq. (2)) is expressed by equating equations (4) and (5):

$$a_1 x_1^{\frac{\beta_1}{2-\beta_1}} = a_2 x_2^{\frac{\beta_2}{2-\beta_2}} \tag{6}$$

The requirement that $\frac{d\bar{U}}{d\bar{x}}$ at $\bar{x}_1$ be equal to $\frac{d\bar{U}}{d\bar{x}}$ at $\bar{x}_2$ (eq. (3)) is expressed by calculating $\left(\frac{dU}{dx}\right)_{x_1}$ from equation (4) and equating it to $\left(\frac{dU}{dx}\right)_{x_2}$ calculated from equation (5). The result is

$$a_2 \frac{\beta_2}{2-\beta_2} x_2^{\frac{2(\beta_2-1)}{2-\beta_2}} = a_1 \frac{\beta_1}{2-\beta_1} x_1^{\frac{2(\beta_1-1)}{2-\beta_1}} \tag{7}$$

When equation (7) is divided by equation (6) the result is

$$\frac{x_2}{x_1} = \frac{\beta_2}{\beta_1}\frac{2 - \beta_1}{2 - \beta_2} \tag{8}$$

where, in order for equation (3) to be satisfied, β_1 and β_2 must be either both positive or both negative. Thus, U and $\frac{dU}{dx}$ at $x = x_2$, in a flow with $\beta = \beta_2$ and $a = a_2$, are equal, respectively, to U and $\frac{dU}{dx}$ at

$$x_1 = x_2 \frac{\beta_1}{\beta_2}\frac{2 - \beta_2}{2 - \beta_1}$$

in a flow with $\beta = \beta_1$ and $a = a_1$. The relation between a_1 and a_2 is obtained by the use of equation (8) and either equation (6) or equation (7). The result is

$$a_2 = a_1 x_1^{\frac{2(\beta_1-\beta_2)}{(2-\beta_1)(2-\beta_2)}}\left(\frac{\beta_1}{\beta_2}\frac{2 - \beta_2}{2 - \beta_1}\right)^{\frac{\beta_2}{2-\beta_2}} \tag{9}$$

Consequently, in the flow over infinite wedges a point on one wedge can have $\bar{U}$ and $\frac{d\bar{U}}{d\bar{x}}$ equal, respectively, to $\bar{U}$ and $\frac{d\bar{U}}{d\bar{x}}$ at a point on a wedge of different angle. The arbitrary quantities a_1, x_1, β_1, and β_2 determine x_2 and a_2 by equations (8) and (9). Fixing the arbitrary quantity a_1 is equivalent to fixing $\bar{U}/\bar{U}_o$ at $\bar{x} = \bar{c}$ in the flow for which $\beta = \beta_1$. The quantity a_2 is not arbitrary but is determined by equation (9); the quantity a_2 is the value of $\bar{U}/\bar{U}_o$ at $\bar{x} = \bar{c}$ on the wedge with $\beta = \beta_2$.

Stability of Laminar-Boundary-Layer Velocity Profiles on Wedges

The assumption concerning the stability of a laminar-boundary-layer velocity profile is the same as in reference 2, namely, that the ratio R_{θ_c}/R_θ at a distance x from the stagnation point is a measure of the stability of the boundary layer at that value of x and that the boundary layer becomes more stable as the ratio R_{θ_c}/R_θ increases. In order to compare the stability of a velocity profile at $x = x_2$ with the stability of a profile at $x = x_1$, it is necessary to find R_θ and R_{θ_c} at both x_1 and x_2.

In order to obtain R_θ the definition for $\bar{\theta}$ is used; the definition is

$$\bar{\theta} = \int_0^\infty \frac{\bar{u}}{\bar{U}}\left(1 - \frac{\bar{u}}{\bar{U}}\right)d\bar{y}$$

The velocity $\bar{u}$ is obtained from the relations

$$\bar{u} = \frac{\partial\bar{\psi}}{\partial\bar{y}}$$

$$\bar{\psi} = \sqrt{2 - \beta}\,\bar{a}^{1/2}\bar{x}^{\frac{1}{2-\beta}}\bar{\nu}^{1/2}F \tag{10}$$

and

$$\bar{y} = \sqrt{2 - \beta}\,\bar{a}^{-1/2}\bar{x}^{\frac{1-\beta}{2-\beta}}\bar{\nu}^{1/2}Y \tag{11}$$

which are from reference 4, pages 139 to 142, but the notation has been changed to that of the present paper.

The result is

$$\bar{u} = \bar{a}\bar{x}^{\frac{\beta}{2-\beta}} F' \tag{12}$$

where the function $F(Y)$ satisfies the differential equation (ref. 4, pp. 139 to 142):

$$F''' + FF'' - \beta\left[(F')^2 - 1\right] = 0 \tag{13}$$

and the boundary conditions

$$Y = 0 \qquad\qquad Y \longrightarrow \infty$$

$$F' = 0,\ F = 0 \qquad\qquad F' \longrightarrow 1$$

When $\beta = 0$, equation (13) becomes the Blasius equation for the flow over a flat plate (ref. 4, p. 135). When equation (12) is used with equation (1) in dimensional form,

$$\bar{U} = \bar{a}\bar{x}^{\frac{\beta}{2-\beta}} \tag{14}$$

the result is

$$\frac{\bar{u}}{\bar{U}} = F' \tag{15}$$

By making use of equations (11), (14), and (15), the expression for $\bar{\theta}$ can be written as

$$\frac{\bar{\theta}}{\bar{x}}\sqrt{\frac{\bar{U}\bar{x}}{\bar{\nu}}} = \sqrt{2 - \beta}\int_0^\infty F'(1 - F')dY \tag{16}$$

The expression for R_θ then is

$$R_\theta = \frac{\bar{U}\bar{\theta}}{\bar{\nu}} = \sqrt{\frac{\bar{U}\bar{x}}{\bar{\nu}}}\sqrt{2-\beta}\int_0^\infty F'(1-F')dY$$

or

$$R_\theta = \sqrt{\frac{\bar{U}_o\bar{c}}{\bar{\nu}}}\sqrt{Ux}\sqrt{2-\beta}\int_0^\infty F'(1-F')dY \tag{17}$$

From equation (1) it follows that

$$Ux = ax^{\frac{2}{2-\beta}}$$

and that

$$\frac{U^2}{\frac{dU}{dx}} = \frac{a^2x^{\frac{2\beta}{2-\beta}}}{a\frac{\beta}{2-\beta}x^{\frac{2(\beta-1)}{2-\beta}}} = \frac{2-\beta}{\beta}ax^{\frac{2}{2-\beta}}$$

Therefore:

$$Ux = \frac{\beta}{2-\beta}\frac{U^2}{\frac{dU}{dx}}$$

Expression (17) for R_θ can thus be written as

$$\frac{R_\theta}{\sqrt{\frac{U^2R_c}{\left|\frac{dU}{dx}\right|}}} = \sqrt{|\beta|}\int_0^\infty F'(1-F')dY \tag{18}$$

The integral $\int_0^\infty F'(1 - F')dY$, a function of β, was calculated from table II of reference 3 by use of Simpson's rule (ref. 6, pp. 120 to 122). All the entries in the table for a specific value of β were used to get the integral for that value of β. The function $\frac{R_\theta}{\sqrt{\frac{U^2R_c}{\left|\frac{dU}{dx}\right|}}}$ is shown in figure 2 and the integral $\int_0^\infty F'(1 - F')dY$ is given in table I. The integral $\int_0^\infty (1 - F')dY$, related to the displacement thickness $\bar{\delta}^*$ by the equation

$$\frac{\bar{\delta}^*}{\bar{x}}\sqrt{\frac{\bar{U}\bar{x}}{\bar{\nu}}} = \sqrt{2 - \beta}\int_0^\infty (1 - F')dY$$

is also given in table I.

In order to find the expression for R_{θ_c}, the conclusion of reference 7 that the critical Reynolds number of a velocity profile depends only on the shape of the velocity profile is used. For wedge flows the shape of the velocity profile depends only on the value of the parameter β (see eq. (13)). Therefore, the critical Reynolds number R_{θ_c} depends only on β:

$$R_{\theta_c} = R_{\theta_c}(\beta)$$

The critical Reynolds number is calculated by Lin's rapid method (ref. 8). The critical Reynolds numbers for some of the velocity profiles given by Hartree in reference 3 have already been calculated by Lin's rapid method and are given in figure 2 of reference 9. Because only the first significant figure of the critical Reynolds number can be read without estimation from this figure and because critical Reynolds numbers were calculated for less than half of the profiles given by Hartree in reference 3, the critical Reynolds numbers are computed in the present work for all the Hartree profiles.

Lin's simplified formula for R_{θ_c} is

$$R_{\theta_c} = \frac{25\left(\frac{\partial \frac{\bar{u}}{\bar{U}}}{\partial \frac{\bar{y}}{\bar{\theta}}}\right)_w}{\left(\frac{\bar{u}_c}{\bar{U}}\right)^4} \tag{19}$$

which is taken from reference 8 but has been put in the notation of the present paper.

This formula is to be put in a form that contains the variables F and Y of equation (13). The use of equations (11), (14), (15), and (16) leads to

$$\left(\frac{\partial \frac{\bar{u}}{\bar{U}}}{\partial \frac{\bar{y}}{\bar{\theta}}}\right) = F'' \int_0^\infty F'(1 - F')dY \tag{20}$$

The term $\bar{u}_c/\bar{U}$ in equation (19) is the value of $\bar{u}/\bar{U}$ for which the relation

$$-\pi\left(\frac{\partial \frac{\bar{u}}{\bar{U}}}{\partial \frac{\bar{y}}{\bar{\theta}}}\right)_w \left[3 - \frac{2\left(\frac{\partial \frac{\bar{u}}{\bar{U}}}{\partial \frac{\bar{y}}{\bar{\theta}}}\right)_w \frac{\bar{y}}{\bar{\theta}}}{\frac{\bar{u}}{\bar{U}}}\right] \frac{\frac{\bar{u}}{\bar{U}} \frac{\partial^2 \frac{\bar{u}}{\bar{U}}}{\partial\left(\frac{\bar{y}}{\bar{\theta}}\right)^2}}{\left(\frac{\partial \frac{\bar{u}}{\bar{U}}}{\partial \frac{\bar{y}}{\bar{\theta}}}\right)^3} = 0.58 \tag{21}$$

(from ref. 8) is satisfied.

From equations (11), (14), and (16) the relation

$$\frac{\bar{y}}{\bar{\theta}} = \frac{Y}{\int_0^\infty F'(1 - F')dY} \tag{22}$$

is obtained.

By using equations (20) and (22) the relation

$$\frac{\partial^2 \frac{\bar{u}}{\bar{U}}}{\partial\left(\frac{\bar{y}}{\bar{\theta}}\right)^2} = F''' \left[\int_0^\infty F'(1 - F')dY\right]^2$$

is obtained.

The equation for $\bar{u}_c/\bar{U}$ (eq. (21)) can now be written as

$$-\pi F_w'' \left(3 - \frac{2F_w'' Y}{F'}\right) \frac{F'F'''}{(F'')^3} = 0.58 \tag{23}$$

and the equation for R_{θ_c} (eq. (19)) can be written as

$$R_{\theta_c} = \frac{25F_w'' \int_0^\infty F'(1 - F')dY}{(F_c')^4} \tag{24}$$

where F_c' is the value of F' for which equation (23) is satisfied.

The values of F_w'' given in table II were taken from Hartree (table II of ref. 3, where F_w'' is called $y''(0)$). The integral $\int_0^\infty F'(1 - F')dY$ has already been computed (see eq. (18) and table I). A detailed description of the computation of F_c' is given in the appendix. For $\beta \geq -0.14$, numerical differentiation of Hartree's tabular values of F' (y' in Hartree's notation) was not used to find F'' and F''' in the equation for F_c' (eq. (23)). Instead, the function F' was expanded from $Y = 0$ in a Taylor's series and the derivatives of F' were found by differentiating the series. This procedure is believed to result in more accurate values of F_c', and hence of R_{θ_c}, than could have been obtained by numerically differentiating Hartree's tabular values to find F'' and F'''. The variation of R_{θ_c} with β, calculated by the equation for R_{θ_c} (eq. (24)), is shown in figure 3. The values of R_{θ_c} are also given in table II.

The ratio R_{θ_c}/R_θ can now be found by dividing equation (24) by equation (18); the result, $\frac{R_{\theta_c}}{R_\theta}\sqrt{\frac{U^2R_c}{\left|\frac{dU}{dx}\right|}}$, is shown as a function of β in figure 4. Figures 2 and 4 can be used to determine whether the flows defined by equation (1) contain points with equal U and $\frac{dU}{dx}$ and with the property that the point with the larger value of θ has the larger value of R_{θ_c}/R_θ; the value of R_c is the same for all the flows. Figure 2 shows that when two points have equal values of R_c, U, and $\frac{dU}{dx}$ but different values of β, the point that has the larger absolute value of β has the larger value of R_θ. It is recalled that because of equation (3) both values of β have the same sign. Figure 4 shows that for points with the same values of R_c, U, and $\frac{dU}{dx}$ the value of R_{θ_c}/R_θ increases with β for $\beta > 0.05$. Therefore, for $\beta > 0.05$ the point with the larger value of R_θ has the larger value of R_{θ_c}/R_θ; thus, of two points with equal values of U and $\frac{dU}{dx}$ in flows with equal R_c, the point with the larger value of θ can have the more stable velocity profile. The exact solutions of the boundary-layer equations for a special type of pressure distribution thus confirm a result of reference 2.

Comparison of Predictions of a Method Based on the Hartree Profiles With Predictions of the Schlichting Method

The purpose of the second part of the present investigation is to determine whether replacing the Schlichting single-parameter family of velocity profiles (ref. 1) by the Hartree single-parameter family of velocity profiles (ref. 3) would leave the conclusions of reference 2 essentially unchanged.

The investigation is made by first determining whether or not an approximate method based on the Hartree velocity profiles predicts that an increase in boundary-layer thickness alone at a point can increase the stability of the boundary layer at that point. The values of R_{θ_c} for the Hartree profiles are then compared with the values of R_{θ_c} for the corresponding Schlichting profiles, and the curve of $\frac{R_{\theta_c}}{R_\theta}\sqrt{\frac{U^2R_c}{\left|\frac{dU}{dx}\right|}}$ for the Hartree profiles is compared with that for the Schlichting profiles.

Of interest also is a comparison of the rate of change of the velocity-profile shape parameter and of the stability parameter $\frac{R_{\theta c}}{R_\theta}\sqrt{\frac{U^2R_c}{\left|\frac{dU}{dx}\right|}}$ with change in boundary-layer thickness. Finally, the rate of change of the local roughness Reynolds number with change in boundary-layer thickness is calculated for the Hartree profiles and compared with that for the Schlichting profiles. In order to set up a method based on the Hartree profiles, only the boundary-layer momentum equation (ref. 4, p. 133) and equation (18) need be used. Equation (18) states that the local value of $\frac{R_\theta}{\sqrt{\frac{U^2R_c}{\left|\frac{dU}{dx}\right|}}}$ determines the local value of β. Positive values of β occur for positive values of $\frac{dU}{dx}$. The determination of β completely determines the local state of the boundary layer. A method based on the Hartree profiles is given in references 10 and 11.

In order to determine whether or not an approximate method based on the Hartree velocity profiles predicts that an increase in boundary-layer thickness alone at a point can increase the value of $R_{\theta c}/R_\theta$ at that point, only figures 2 and 4 need be used. In figure 2 is shown the connection between β and $\frac{R_\theta}{\sqrt{\frac{U^2R_c}{\left|\frac{dU}{dx}\right|}}}$; the figure shows that β increases as $\frac{R_\theta}{\sqrt{\frac{U^2R_c}{\left|\frac{dU}{dx}\right|}}}$ increases when β is positive. Therefore, β increases as θ increases, when β is positive and R_c, U, and $\frac{dU}{dx}$ are fixed. Figure 4 shows how the stability parameter $\frac{R_{\theta c}}{R_\theta}\sqrt{\frac{U^2R_c}{\left|\frac{dU}{dx}\right|}}$ depends on β; for $\beta > 0.05$ an increase in β increases $\frac{R_{\theta c}}{R_\theta}\sqrt{\frac{U^2R_c}{\left|\frac{dU}{dx}\right|}}$. Hence, an increase in θ, with R_c, U, and $\frac{dU}{dx}$ fixed, results in an increase in β, and consequently, for $\beta > 0.05$, in an increase in $R_{\theta c}/R_\theta$. On

the other hand, the combination of figures 2 and 4 shows that when $0 < \beta < 0.05$ a small increase in θ results in a decrease in R_{θ_c}/R_θ. This behavior is the same as that found in reference 2.

In order to compare the curves for R_{θ_c} and $\frac{R_{\theta_c}}{R_\theta}\sqrt{\frac{U^2R_c}{\left|\frac{dU}{dx}\right|}}$ obtained in reference 2 as functions of the Schlichting velocity-profile parameter K with the curves for R_{θ_c} and $\frac{R_{\theta_c}}{R_\theta}\sqrt{\frac{U^2R_c}{\left|\frac{dU}{dx}\right|}}$ obtained in the present investigation as functions of β, both K and β are replaced by a parameter called κ by Schlichting (ref. 1) and k in reference 2. The parameter k is the value of the nondimensional pressure gradient (ref. 2):

$$k = \frac{R_\theta^2}{R_c}\frac{1}{U^2}\frac{dU}{dx} \tag{25}$$

The relation between β and k can be obtained by combining equations (18) and (25); the result is

$$k = \beta\left[\int_0^\infty F'(1 - F')dY\right]^2 \tag{26}$$

The relation between K and k is (ref. 2)

$$k = g^2(K + 1) \qquad (k_1 = 0) \tag{27}$$

Therefore, the value of β and the value of K that occur together for any value of k satisfy the equation obtained from equation (26) and equation (27); thus,

$$g^2(K + 1) - \beta\left[\int_0^\infty F'(1 - F')dY\right]^2 = 0$$

where

$$g = C_o + C_1K + C_2K^2$$

The values of C_o, C_1, and C_2 are given in reference 1. The values of β and K that occur together are therefore given by the equation

$$\left(C_o + C_1K + C_2K^2\right)^2(K + 1) - \beta\left[\int_0^\infty F'(1 - F')dY\right]^2 = 0 \qquad (28)$$

For each value of β for which Hartree gives a velocity profile (ref. 3) the corresponding value of K was found from equation (28) by a process of successive approximation. The variation of β and K with the nondimensional pressure gradient k is given in table III and in figure 5. Figure 6 gives the variation of R_{θ_c} with k for the Hartree profiles and for the Schlichting profiles. Figure 7 shows how $\frac{R_{\theta_c}}{R_\theta}\sqrt{\frac{U^2R_c}{\left|\frac{dU}{dx}\right|}}$ for both the Hartree and the Schlichting profiles depends on k. Because the abscissa k in figures 6 and 7 is a function of β alone, figures 6 and 7 can also be interpreted as a comparison between the exact values of R_{θ_c} and $\frac{R_{\theta_c}}{R_\theta}\sqrt{\frac{U^2R_c}{\left|\frac{dU}{dx}\right|}}$ for wedges and the approximate values of R_{θ_c} and $\frac{R_{\theta_c}}{R_\theta}\sqrt{\frac{U^2R_c}{\left|\frac{dU}{dx}\right|}}$ calculated for these wedges by making use of Schlichting's method (ref. 1).

In order to find how $d\beta/dR_\theta$, the rate of change of profile shape parameter with change in boundary-layer thickness, depends on β, equation (18) is used. The result for $R_\theta \frac{\partial\beta}{\partial R_\theta}$ is

$$R_\theta \frac{\partial\beta}{\partial R_\theta} = \frac{\beta}{\frac{\beta}{\int_0^\infty F'(1 - F')dY}\frac{d}{d\beta}\int_0^\infty F'(1 - F')dY + \frac{1}{2}} \qquad (29)$$

The quantity $\int_0^\infty F'(1 - F')dY$ has already been calculated. In order to calculate $\frac{d}{d\beta}\int_0^\infty F'(1 - F')dY$, a table of divided differences was formed with β as the independent variable. The derivative $\frac{d}{d\beta}\int_0^\infty F'(1 - F')dY$ was found from the table by use of the formula of example 4, page 217 of reference 6. The function $R_\theta \frac{\partial\beta}{\partial R_\theta}$ is shown in figure 8. In the same figure is shown $R_\theta \frac{\partial K}{\partial R_\theta}$ for the Schlichting profiles, taken from reference 2. Although the ratio of $R_\theta \frac{\partial\beta}{\partial R_\theta}$ to $R_\theta \frac{\partial K}{\partial R_\theta}$ becomes large as k departs from zero, the rate of change of $\frac{R_{\theta_c}}{R_\theta}\sqrt{\frac{U^2R_c}{\left|\frac{dU}{dx}\right|}}$ with R_θ (really θ) is about the same for the Schlichting and Hartree profiles for most of the range of k; thus

$$R_\theta \frac{d\left(\frac{R_{\theta_c}}{R_\theta}\sqrt{\frac{U^2R_c}{\left|\frac{dU}{dx}\right|}}\right)}{dR_\theta} = R_\theta \frac{d\left(\frac{R_{\theta_c}}{R_\theta}\sqrt{\frac{U^2R_c}{\left|\frac{dU}{dx}\right|}}\right)}{dk}\frac{dk}{dR_\theta}$$

but

$$k = \frac{R_\theta^2}{R_c}\frac{1}{U^2}\frac{dU}{dx}$$

therefore

$$R_\theta \frac{dk}{dR_\theta} = 2k \qquad (R_c,\ U, \text{ and } \frac{dU}{dx} \text{ fixed})$$

and

$$R_\theta \frac{d\left(\frac{R_{\theta_c}}{R_\theta}\sqrt{\frac{U^2R_c}{\left|\frac{dU}{dx}\right|}}\right)}{dR_\theta} = 2k \frac{d\left(\frac{R_{\theta_c}}{R_\theta}\sqrt{\frac{U^2R_c}{\left|\frac{dU}{dx}\right|}}\right)}{dk} \tag{30}$$

Because figure 7 shows $\frac{d\left(\frac{R_{\theta_c}}{R_\theta}\sqrt{\frac{U^2R_c}{\left|\frac{dU}{dx}\right|}}\right)}{dk}$ to be about the same for both the Hartree and the Schlichting velocity profiles over most of the range of k, it follows from equation (30) that the rate of change of $\frac{R_{\theta_c}}{R_\theta}\sqrt{\frac{U^2R_c}{\left|\frac{dU}{dx}\right|}}$ with θ is also about the same for the Hartree and Schlichting profiles. In the region near $k = 0.015$, however, there are differences; the derivative $R_\theta \frac{d\left(\frac{R_{\theta_c}}{R_\theta}\sqrt{\frac{U^2R_c}{\left|\frac{dU}{dx}\right|}}\right)}{dR_\theta}$ is positive for the Hartree profiles for values of k for which it is negative for the Schlichting profiles.

The effect of an increase in boundary-layer thickness on the roughness Reynolds number R_h is obtained by substituting the expression

$$F_w'' \int_0^\infty F'(1 - F')dY$$

for the term $f(K)$ in equation (16) of reference 2. The equation for $\frac{R_\theta}{R_h}\frac{\partial R_h}{\partial R_\theta}$ for the Hartree profiles becomes, after a development parallel to that of reference 2,

$$\frac{R_\theta}{R_h}\frac{\partial R_h}{\partial R_\theta} = -1 + R_\theta \frac{\partial \beta}{\partial R_\theta}\left[\frac{d}{d\beta} F_w'' \int_0^\infty F'(1 - F')dY\right] \frac{1}{F_w'' \int_0^\infty F'(1 - F')dY} \tag{31}$$

Figure 9 shows how $\frac{R_\theta}{R_h}\frac{\partial R_h}{\partial R_\theta}$ varies with the nondimensional pressure gradient k for both the Hartree and the Schlichting velocity profiles; the values for the Schlichting profiles are taken from reference 2. The use of either the Hartree or the Schlichting velocity profiles leads to the conclusion that an increase in boundary-layer thickness decreases the roughness Reynolds number.

The information contained in figures 6 to 9 indicates that a method based on the Hartree profiles should predict essentially the same effects of an increase in boundary-layer thickness as the calculations of reference 2, which made use of the Schlichting method. For example, a calculation made by the Schlichting method predicts that if the value of θ at 35 percent of the chord from the leading edge of the NACA 64A010 airfoil at a Reynolds number of 10^7 is multiplied by 3.45, the value of R_θ is increased from 1,221 to 4,208 and the value of R_{θ_c}/R_θ is increased from 0.239 to 1.0 (see p. 23 of ref. 2). A calculation made by the use of the information for the Hartree profiles in figure 7 predicts that this value of θ should be multiplied by 3.27 to increase R_{θ_c}/R_θ from 0.210 to 1.0; the value of R_θ is increased from 1,221 to 4,000. (The value of $\sqrt{\frac{U^2R_c}{\left|\frac{dU}{dx}\right|}}$ at this position of the airfoil for $R_c = 10^7$ is equal to 14,260.)

DISCUSSION

The numerical solutions of the boundary-layer equations for the flow over infinite wedges are used to show that a thick velocity profile on one wedge can be more stable than a thin profile on another wedge, although the velocity outside the boundary layer and the pressure gradient along the surface are the same for both profiles. A result of the calculations of reference 2, which were based on the approximate Schlichting method, is thus confirmed for a special type of flow.

It is noted, however, that the wedge flows defined by equation (1) satisfy a basic assumption of the Schlichting method, namely, that the velocity-profile shape at any point on the surface, for no flow through the surface, is determined by the value of k at that point. Equation (26) shows that for wedge flows the shape of the velocity profile

is indeed a function of k only. For these flows k is independent of x and depends only on the wedge angle; for a fixed wedge angle there is thus no change in k or in velocity profile along x. On the other hand, in regions in which k varies rapidly along the surface and in which, consequently, the basic assumption of the Schlichting method that the velocity-profile shape depends only on k is not satisfied, the predictions of the Schlichting method will probably be less precise than for the wedge flows. For example, a discontinuity in the distribution of k cannot result in a discontinuous change in the shape of the velocity profile. The profile shape predicted by the Schlichting method can, however, be expected, in a region of falling pressure, gradually to approach a shape that is in the neighborhood of the correct one as the distance downstream from the discontinuity in k is increased.

The result of the second portion of the analysis is that a method for the calculation of the boundary layer based on the Hartree profiles should indicate essentially the same effects of an increase in boundary-layer thickness as the calculations of reference 2, which were based on the Schlichting method. This result makes the conclusions of reference 2 appear to be less dependent on the particular single-parameter family of velocity profiles chosen by Schlichting; one of the weaknesses of the analysis of reference 2 is that it is based on a particular single-parameter family of velocity profiles and that R_{θ_c} is sensitive to the shape of a velocity profile.

CONCLUSIONS

The result is obtained that in flows over infinite wedges cases occur for which a thick boundary-layer velocity profile on one wedge is more stable than a thinner profile on a wedge of different angle, although the velocity outside the boundary layer and the pressure gradient are the same for both profiles. This result confirms a conclusion previously reached by the use of Schlichting's approximate analysis, namely, that in a region of falling pressure the stability of a thick velocity profile can be greater than that of a thin profile when the velocity at the edge of the boundary layer and the pressure gradient are the same for both profiles.

The investigation also leads to the inference that the calculated effects of a change in boundary-layer thickness on the stability and on the local roughness Reynolds number should be essentially unchanged by

replacing the Schlichting single-parameter family of velocity profiles by the Hartree single-parameter family of velocity profiles.

Langley Aeronautical Laboratory,
National Advisory Committee for Aeronautics,
Langley Field, Va., May 11, 1953.

APPENDIX

CALCULATION OF F_c' AND R_{θ_c}

In order to compute F_c' it is necessary first to compute F'' and F''' over a range of Y large enough for equation (23) to be satisfied at one point in this range. The computation of F'' and F''' was made by first expanding the function F' in a Taylor's series from $Y = 0$; the series, to Y^{13}, is

$$F' = \sum_{n=1}^{14} \frac{F_w^n Y^{n-1}}{(n-1)!} \tag{32}$$

where F_w^n means the nth derivative of F at $Y = 0$. The derivative of the series for F' results in the series for F'':

$$F'' = \sum_{n=2}^{14} \frac{F_w^n Y^{n-2}}{(n-2)!} \tag{33}$$

and the derivative of the series for F'' results in the series for F''':

$$F''' = \sum_{n=3}^{14} \frac{F_w^n Y^{n-3}}{(n-3)!} \tag{34}$$

The coefficients F_w^n are obtained by successively differentiating equation (13) and using the boundary conditions at $Y = 0$. Thus, directly from equation (13) and the conditions

$$Y = 0 \qquad F = 0 \qquad F' = 0$$

there results:

$$F_w''' = -\beta$$

The first derivative of equation (13) is

$$F^{IV} + FF''' + F'F''(1 - 2\beta) = 0$$

The boundary conditions at $Y = 0$ then lead to

$$F_w^{IV} = 0$$

This process was repeated over and over until F_w^{XIV} was obtained. The coefficients are listed in table IV. The quantity F_w'' depends only on β and is listed in table II; these values of F_w'' were taken from reference 3 (where the symbol $y''(0)$ was used instead of F_w'').

The series (32), (33), and (34) were used to calculate F', F'', and F''' by using the value of F_w'' given by Hartree (ref. 3) for each value of β. For $\beta \geq 0$, the series (32), (33), and (34) were assumed to be valid representations of F', F'', and F''' from $Y = 0$ to the largest value of Y at which the magnitude of the last term in the series for F''' was less than 0.00005. For $\beta = -0.10$ the criterion was relaxed to allow 0.00008, and for $\beta = -0.14$ the value 0.00013 was allowed. For values of Y less than the largest values of Y at which these requirements were satisfied, the values of F' calculated by the series (32) did not show a consistent departure from Hartree's tabulated values (ref. 3).

In order to calculate Y_c, the value of Y at which equation (23) is satisfied, equations (33) and (34) and the values of F_w'' and F' given by Hartree (ref. 3) were used to calculate the left-hand side of equation (23), called ϕ, for a range of Y large enough to include values of ϕ greater than 0.58. For values of $-0.14 \leq \beta \leq 2.4$, the computation of Y_c and F_c' then consisted of an iteration procedure in which Y_c was first estimated by applying a divided-difference

method (ref. 6, ch. 7) to the calculated values of ϕ. A new value of ϕ for this value of Y_c was computed by calculating F', F", and F"' for this value of Y from equations (32), (33), and (34). If ϕ was not equal to 0.58 the procedure was repeated and use was made of the new values of ϕ and Y in the divided-difference procedure. This iteration procedure resulted in values of Y_c for which ϕ was equal to 0.5800 ± 0.0001 for all values of β for which $-0.14 \leq \beta \leq 2.4$. The last iteration for Y_c also gave the final value of F_c'.

For $\beta = -0.16$, -0.18, and -0.19 the Taylor's series is not valid to Y_c. In these cases the values of F' in Hartree's table (ref. 3) were used to form difference tables. In most cases third differences were used. These difference tables were used with Newton's and Gauss' formulas (ref. 6, pp. 160 to 170) to compute the values of F" and F"'. The values of F" and F"' computed by the Newton and Gauss formulas were smoothed by one application of the 7-point formula on page 278 of reference 6. These smoothed values of F" and F"' were used with Hartree's tabular values for F' (ref. 3) to compute ϕ. The value of Y for $\phi = 0.58$ was then found by inverse interpolation, for which a divided-difference formula was used (ref. 6). For this value of Y, called Y_c, the value of F', called F_c', was found by interpolation from the difference tables; third differences were used.

Once F_c' was calculated, the critical Reynolds number was computed from the equation for R_{θ_c} (eq. (24)). The variation of R_{θ_c} with β is shown in figure 3. The values of R_{θ_c} are also given in table II, together with Hartree's values (ref. 3) of F_w''. The values of R_{θ_c} in table II are believed to be accurate to about 6 in 10,000 for $-0.14 \leq \beta \leq 2.4$. This estimate of the accuracy is based on an estimate of the effect on the calculated value of R_{θ_c} of a small difference in ϕ from 0.5800. For $\beta \leq -0.16$ the values of R_{θ_c} are probably accurate to the number of significant figures given in the table. These estimates of the accuracy concern only the numerical procedure and do not include the effects on R_{θ_c} of any inexactness in Hartree's values of F_w'' or of any inexactness in Lin's formula (eq. (19)).

In the course of the computations it was noted that the value 0.8860 at $x = 1.6$ (Hartree's notation, ref. 3) and $\beta = 0.5$ did not seem to be consistent with neighboring values. An interpolation which made use of the other values in the vicinity gave 0.8760 instead of 0.8860. The value 0.8760 was used in the computations of the present analysis.

REFERENCES

1. Schlichting, H.: An Approximate Method for Calculation of the Laminar Boundary Layer With Suction for Bodies of Arbitrary Shape. NACA TM 1216, 1949.

2. Tetervin, Neal, and Levine, David A.: A Study of the Stability of the Laminar Boundary Layer As Affected by Changes in the Boundary-Layer Thickness in Regions of Pressure Gradient and Flow Through the Surface. NACA TN 2752, 1952.

3. Hartree, D. R.: On an Equation Occurring in Falkner and Skan's Approximate Treatment of the Equations of the Boundary Layer. Proc. Cambridge. Phil. Soc., vol. XXXIII, pt. 2, Apr. 1937, pp. 223-239.

4. Fluid Motion Panel of the Aeronautical Research Committee and Others: Modern Developments in Fluid Dynamics. Vol. I, S. Goldstein, ed., The Clarendon Press (Oxford), 1938.

5. Falkner, V. M.: A Further Investigation of Solutions of the Boundary Layer Equations. R. & M. No. 1884, British A.R.C., 1937.

6. Milne, William Edmund: Numerical Calculus. Princeton Univ. Press, 1949.

7. Pretsch, J.: Die Stabilität einer ebenen Laminarströmung bei Druckgefälle und Druckanstieg. Jahrb. 1941 der deutschen Luftfahrtforschung, R. Oldenbourg (Munich), pp. I 158 - I 175.

8. Lin, C. C.: On the Stability of Two-Dimensional Parallel Flows. Part III.- Stability in a Viscous Fluid. Quarterly Appl. Math., vol. III, no. 4, Jan. 1946, pp. 277-301.

9. Hahneman, Elizabeth, Freeman, J. C., and Finston, M.: Stability of Boundary Layers and of Flow in Entrance Section of a Channel. Jour. Aero. Sci., vol. 15, no. 8, Aug. 1948, pp. 493-496.

10. Kochin, N. E., and Loytzansky, L. G.: An Approximate Method of Calculating the Laminar Boundary Layer. Comptes Rendus Acad. Sci. USSR, vol. XXXVI, no. 9, 1942, pp. 262-266.

11. Seban, R. A.: Calculation Method for Two Dimensional Laminar Boundary Layers With Arbitrary Free Stream Velocity Variation and Arbitrary Wall Temperature Variation. ATI No. 112297, Univ. Calif., Inst. Eng. Res. (Contract No. W33-038-ac-15229), May 10, 1950.

TABLE I

THE INTEGRALS $\int_0^\infty F'(1 - F')dY$ AND $\int_0^\infty (1 - F')dY$ FOR VARIOUS VALUES OF β

β	$\int_0^\infty F'(1 - F')dY$	$\int_0^\infty (1 - F')dY$
2.4	0.2149	0.4607
2.0	.2308	.4974
1.6	.2502	.5439
1.2	.2760	.6068
1.0	.2923	.6479
.8	.3119	.6987
.6	.3358	.7638
.5	.3502	.8044
.4	.3667	.8526
.3	.3858	.9109
.2	.4080	.9838
.1	.4354	1.0803
0	.4695	1.2167
-.10	.5155	1.4436
-.14	.5388	1.5967
-.16	.5523	1.7076
-.18	.5676	1.8712
-.19	.5768	2.0070
-.1988	.5852	2.3587

TABLE II

THE QUANTITIES F_w'' AND R_{θ_c} FOR VARIOUS VALUES OF β

β	F_w'' (1)	R_{θ_c}
2.4	1.837	6,590
2.0	1.687	6,209
1.6	1.521	5,728
1.2	1.336	5,002
1.0	1.2326	4,529
.8	1.120	3,928
.6	.9960	3,132
.5	.9277	2,662
.4	.8542	2,134
.3	.7748	1,551
.2	.6869	963.0
.1	.5870	470.4
0	.4696	179.5
-.10	.3191	62.3
-.14	.2395	38.4
-.16	.1905	30
-.18	.1285	17
-.19	.086	7
-.1988	0	------

[1]From Hartree's table (ref. 3).

TABLE III

THE VELOCITY-PROFILE PARAMETERS β AND K FOR VARIOUS VALUES OF THE PRESSURE-GRADIENT PARAMETER k

k	β	K
0.1108	2.4	-0.4818
.1067	2.0	-.4986
.1002	1.6	-.5237
.09142	1.2	-.5592
.08542	1.0	-.5839
.07781	.8	-.6159
.06764	.6	-.6597
.06131	.5	-.6877
.05379	.4	-.7217
.04465	.3	-.7644
.03329	.2	-.8196
.01896	.1	-.8934
0	0	-1
-.02658	-.10	-1.176
-.04064	-.14	-1.289
-.04881	-.16	-1.366
-.05800	-.18	-1.470
-.06321	-.19	-1.543
-.06810	-.1988	-1.629

TABLE IV

COEFFICIENTS IN THE TAYLOR'S SERIES FOR F', F", AND F"'

$$F_w''' = -\beta$$

$$F_w^{IV} = 0$$

$$F_w^{V} = -(F_1'')^2(1 - 2\beta)$$

$$F_w^{VI} = 2F_1''\beta(2 - 3\beta)$$

$$F_w^{VII} = -2\beta^2(2 - 3\beta)$$

$$F_w^{VIII} = (F_1'')^3(1 - 2\beta)(11 - 10\beta)$$

$$F_w^{IX} = -2(F_1'')^2\beta(45 - 113\beta + 66\beta^2)$$

$$F_w^{X} = 16F_1''\beta^2(2 - 3\beta)(8 - 7\beta)$$

$$F_w^{XI} = -(F_1'')^4(1 - 2\beta)\left[(29 - 16\beta)(11 - 10\beta) + 14(1 - 2\beta)(4 - 5\beta)\right] - 16\beta^3(8 - 7\beta)(2 - 3\beta)$$

$$F_w^{XII} = (F_1'')^3\beta\left[2(37 - 18\beta)(45 - 113\beta + 66\beta^2) + (1 - 2\beta)(11 - 10\beta)(93 - 72\beta)\right]$$

$$F_w^{XIII} = -2(F_1'')^2\beta^2\left[16(23 - 10\beta)(2 - 3\beta)(8 - 7\beta) + 10(13 - 9\beta)(45 - 113\beta + 66\beta^2) + 6(27 - 28\beta)(1 - 2\beta)(2 - 3\beta)\right]$$

$$F_w^{XIV} = (F_1'')^5\left\{2(28 - 11\beta)(1 - 2\beta)\left[(29 - 16\beta)(11 - 10\beta) + 14(1 - 2\beta)(4 - 5\beta)\right] + 3(139 - 136\beta)(1 - 2\beta)^2(11 - 10\beta)\right\} + 8F_1''\beta^3\left[4(28 - 11\beta)(8 - 7\beta)(2 - 3\beta) + 44(8 - 5\beta)(2 - 3\beta)(8 - 7\beta) + 3(27 - 28\beta)(2 - 3\beta)^2\right]$$

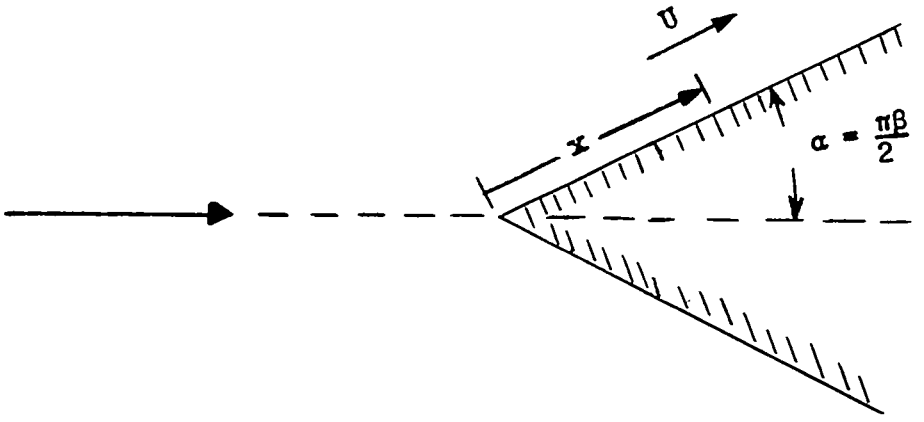

(a) $\beta \geqq 0$.

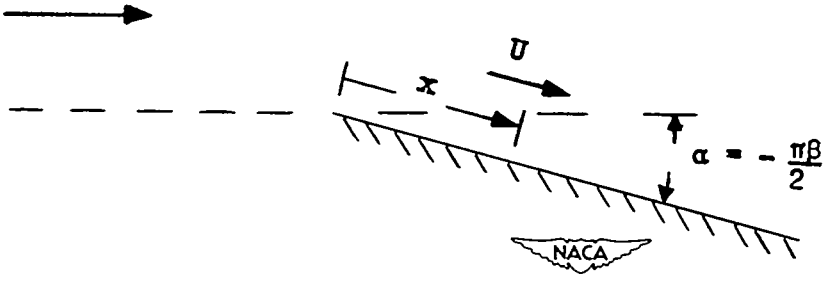

(b) $\beta < 0$.

Figure 1.- Flow over the walls of a wedge.

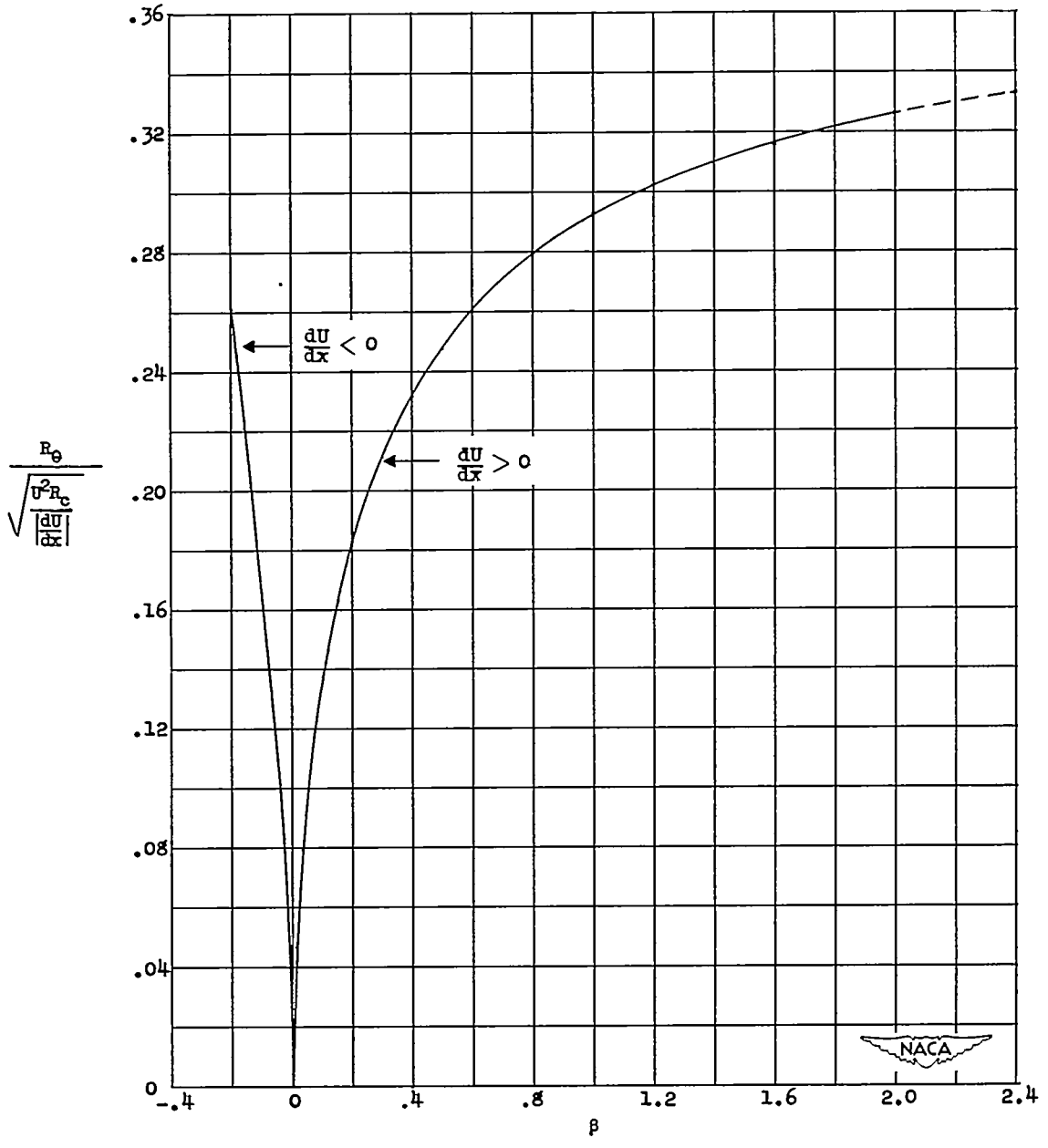

Figure 2.- Variations of the boundary-layer Reynolds number parameter $R_\theta \Big/ \sqrt{\frac{U^2R_c}{\left|\frac{dU}{dx}\right|}}$ with the velocity-profile shape parameter β.

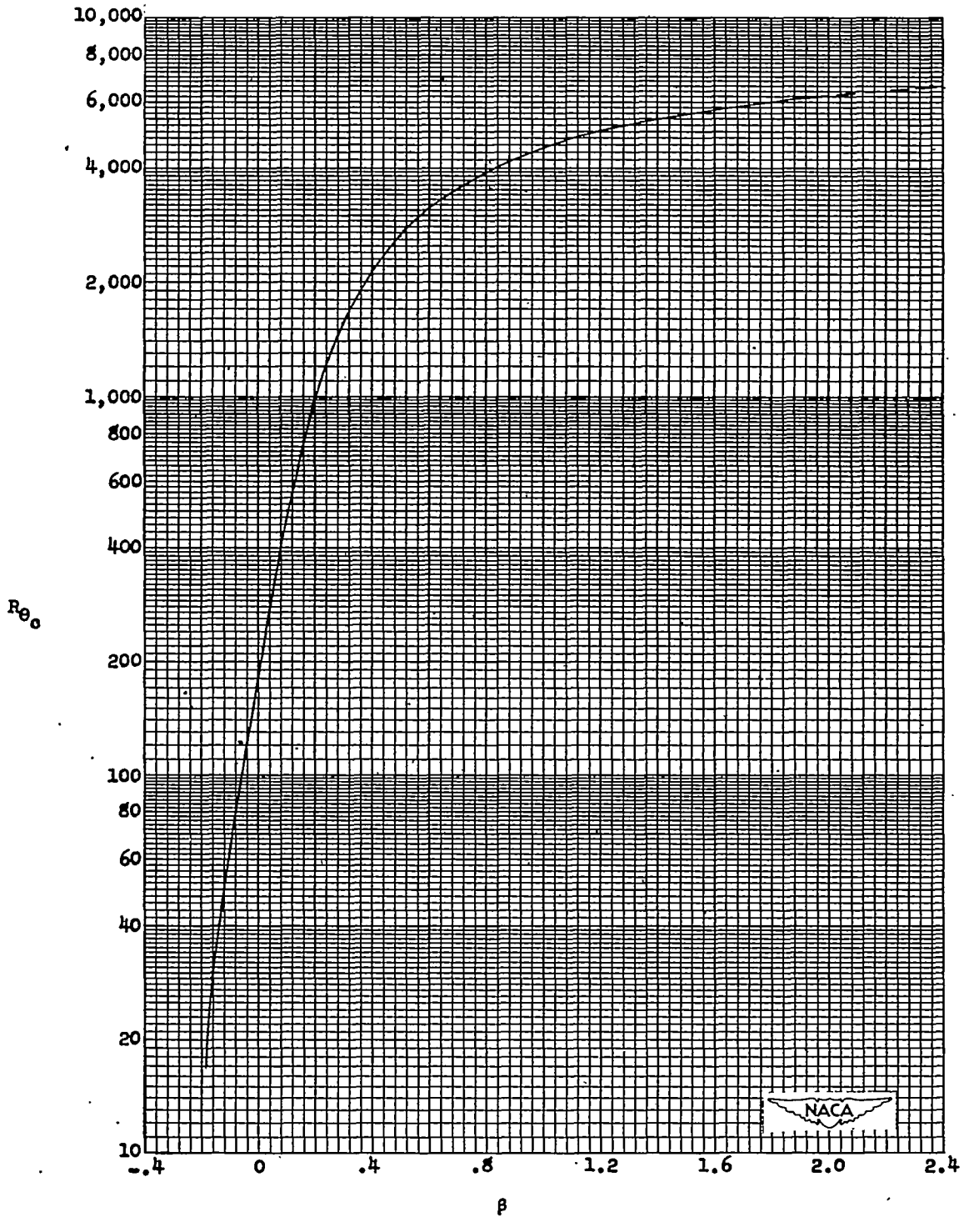

Figure 3.- Variation of the critical boundary-layer Reynolds number R_{θ_c} with the velocity-profile shape parameter β.

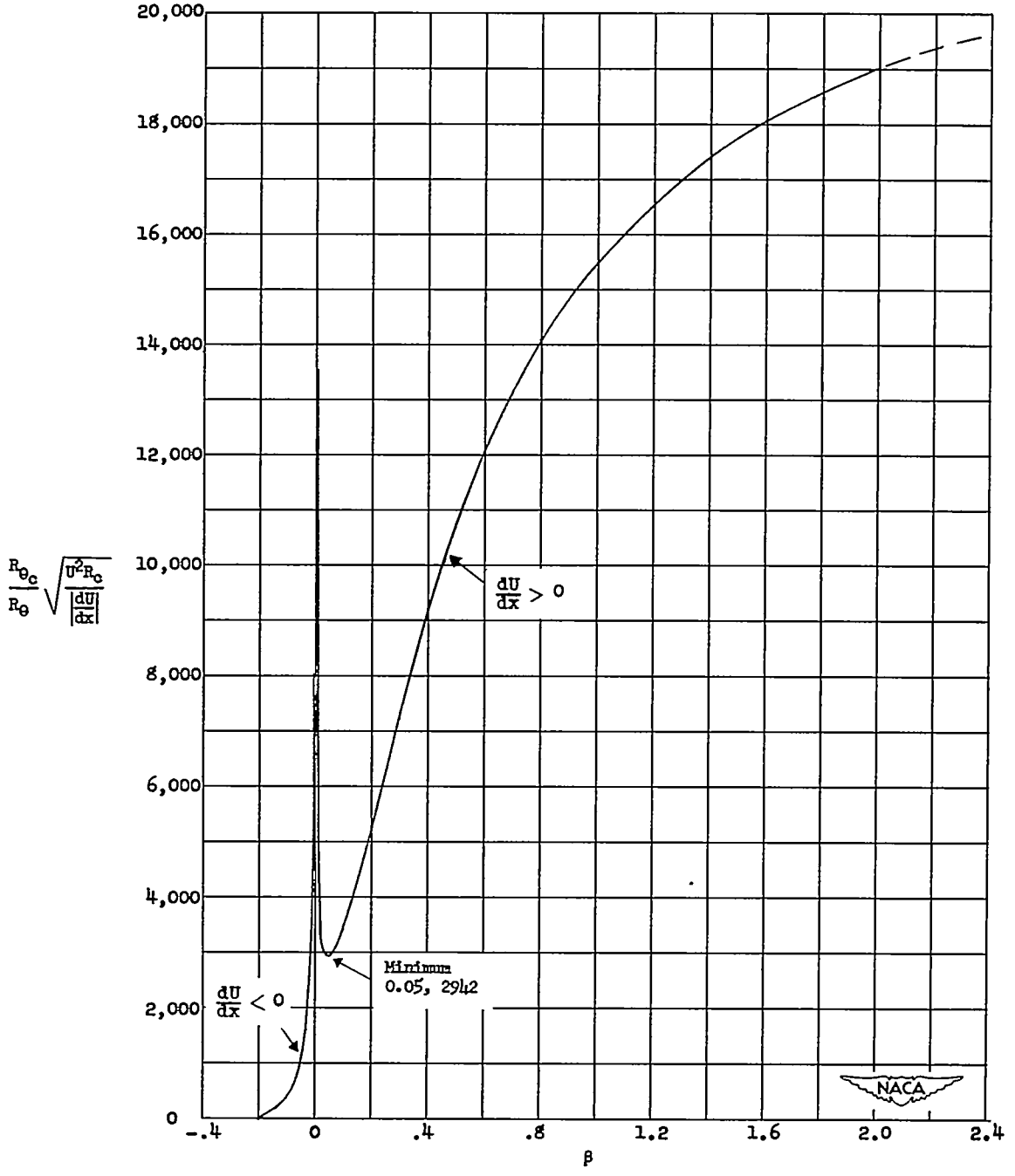

Figure 4.- Variation of $\frac{R_{\theta_c}}{R_\theta}\sqrt{\frac{U^2R_c}{\left|\frac{dU}{dx}\right|}}$, the boundary-layer stability parameter, with the velocity-profile shape parameter β.

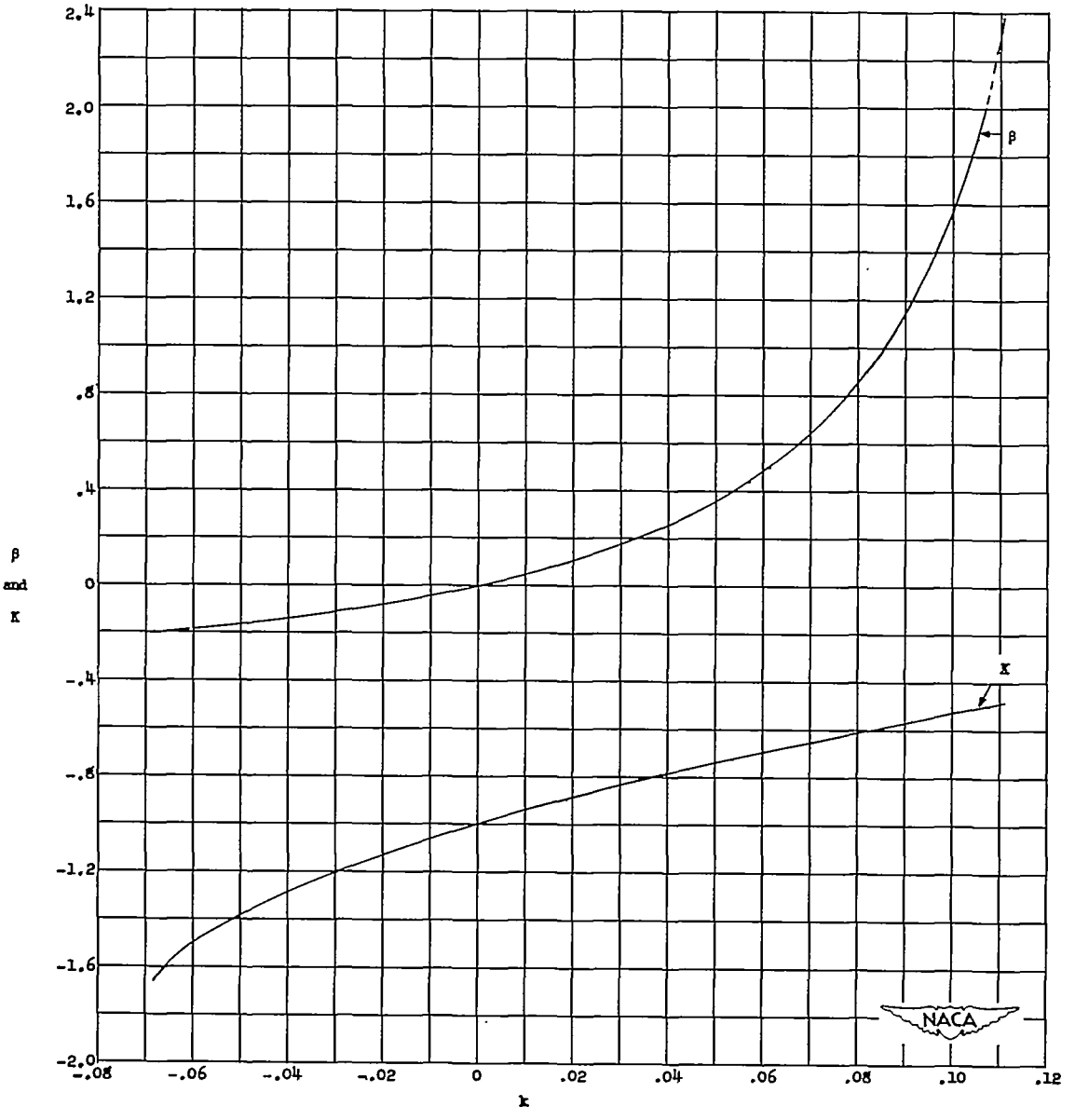

Figure 5.- Variation of the velocity-profile shape parameters β and K with the nondimensional pressure gradient k.

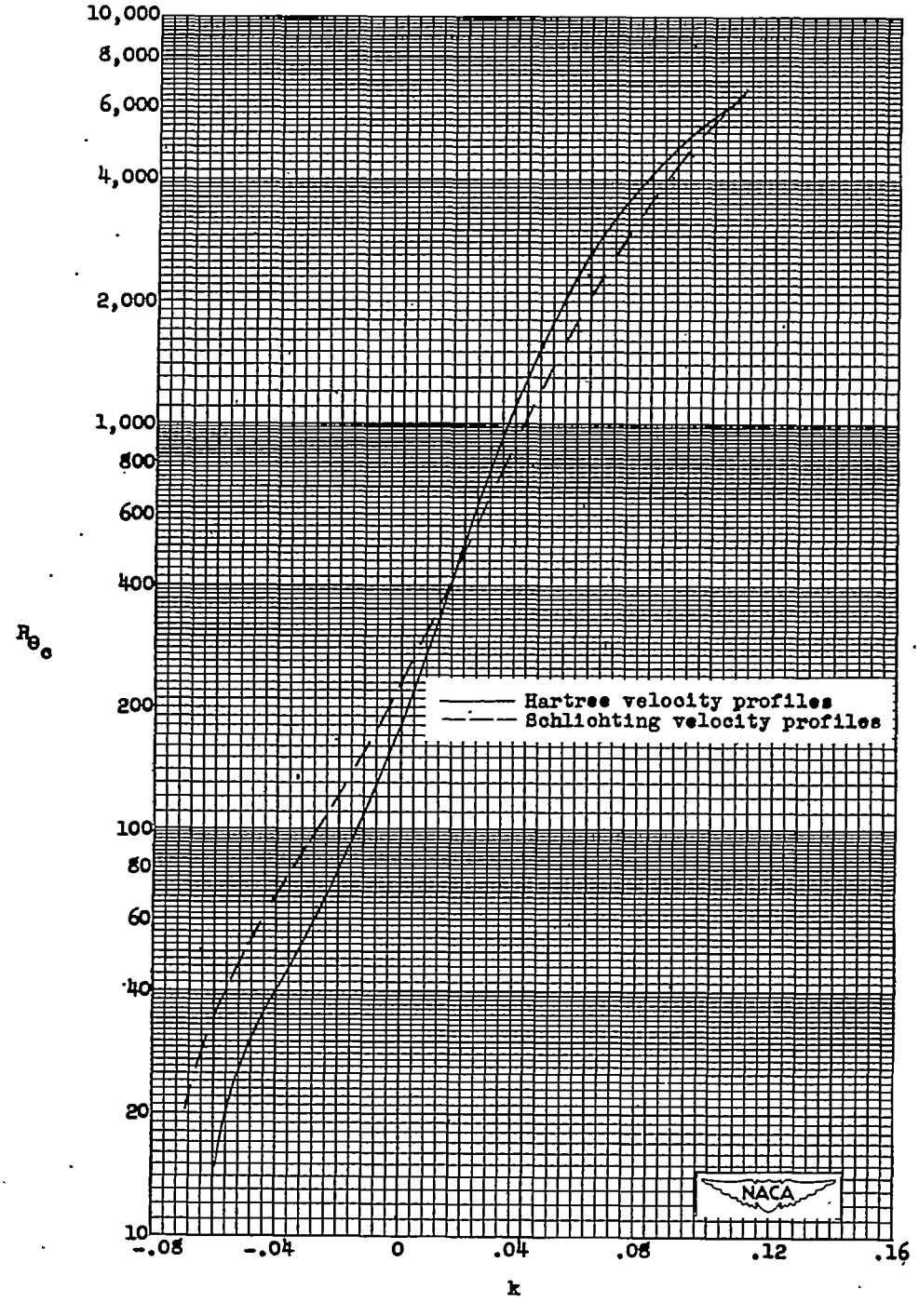

Figure 6.- Variation of the critical boundary-layer Reynolds number R_{θ_c} with the nondimensional pressure-gradient parameter k for the Hartree and the Schlichting velocity profiles. $k = \frac{R_\theta^2}{R_c} \frac{1}{U^2} \frac{dU}{dx}$.

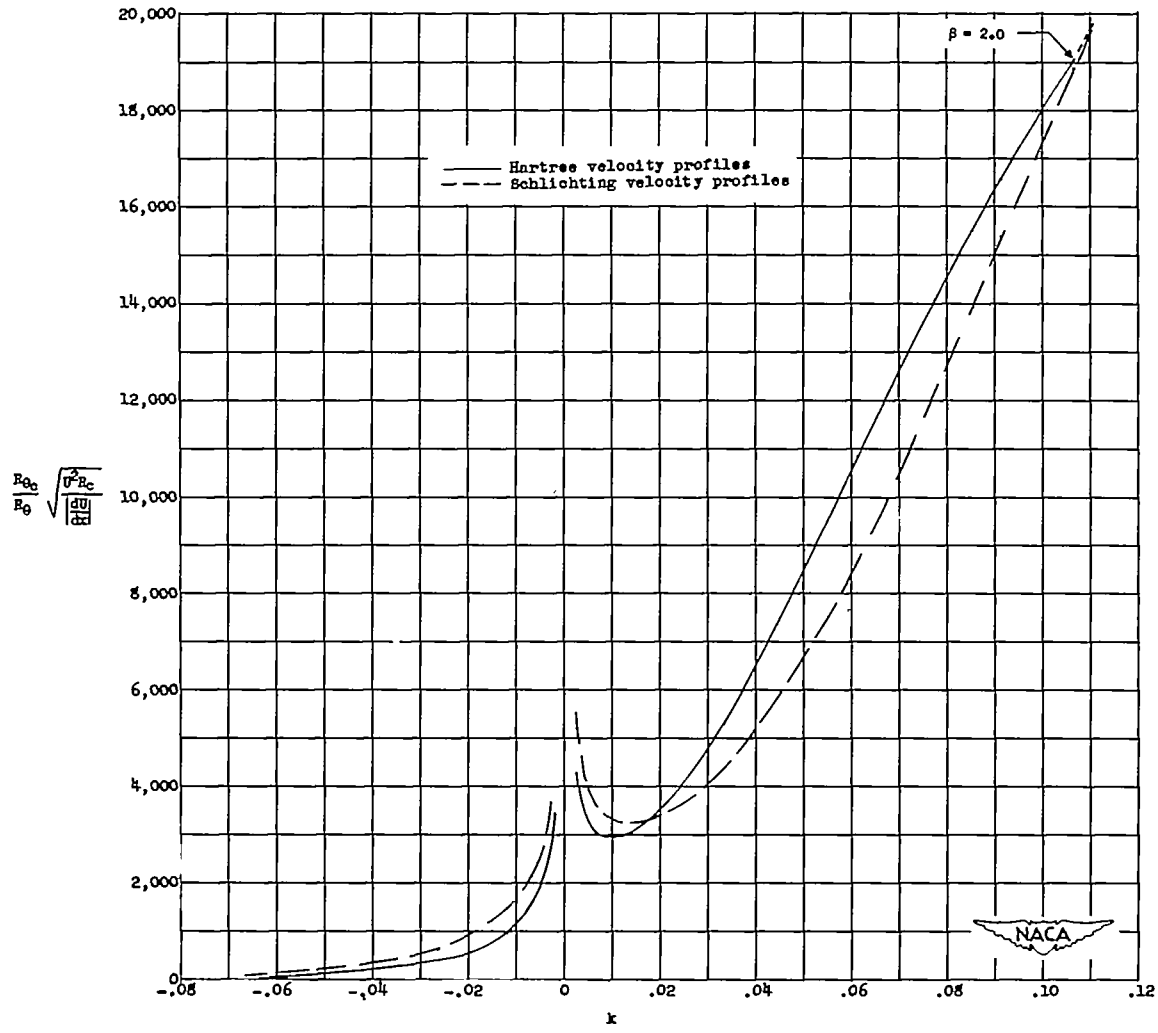

Figure 7.- Variation of $\frac{R_{\theta_c}}{R_\theta}\sqrt{\frac{U^2R_c}{\left|\frac{dU}{dx}\right|}}$, the boundary-layer stability parameter, with the nondimensional pressure-gradient parameter k for the Hartree and the Schlichting velocity profiles.

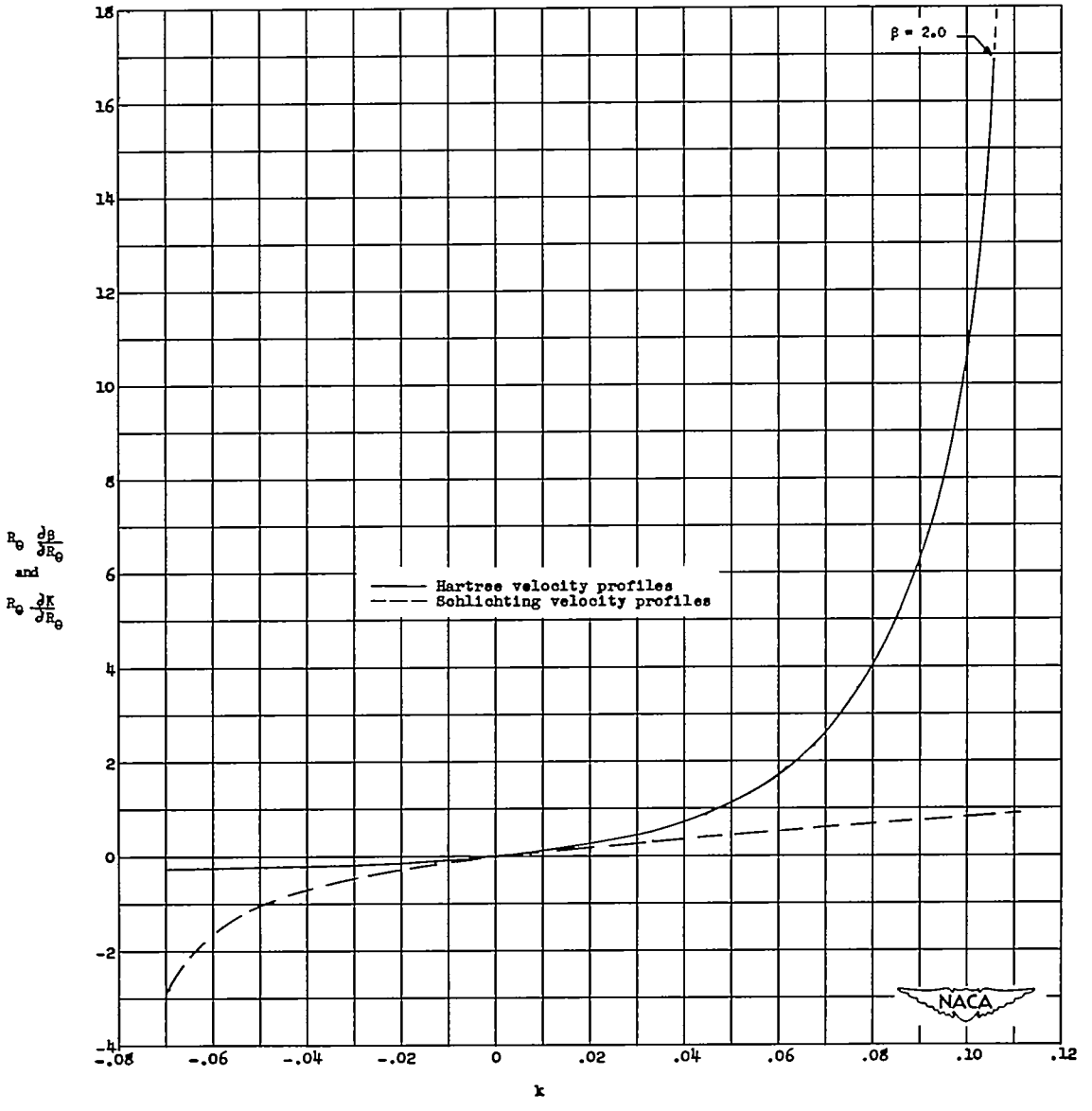

Figure 8.- Variation with the nondimensional pressure gradient k of $R_\theta \frac{\partial \beta}{\partial R_\theta}$, the parameter for rate of change of β with boundary-layer thickness, and of $R_\theta \frac{\partial K}{\partial R_\theta}$, the parameter for rate of change of K with boundary-layer thickness.

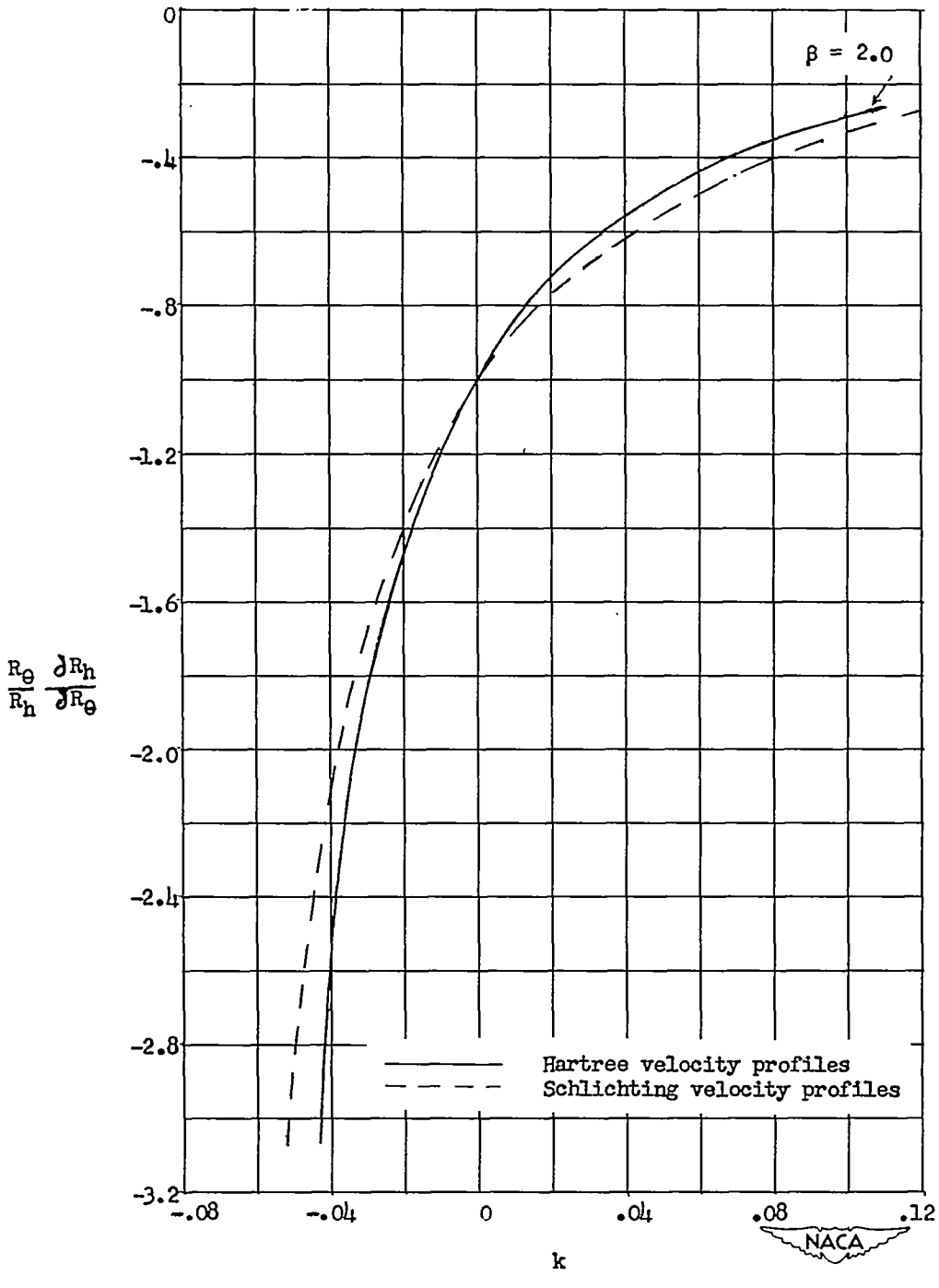

Figure 9.- Variation with the nondimensional pressure gradient k of $\frac{R_\theta}{R_h}\frac{\partial R_h}{\partial R_\theta}$, the parameter for rate of change of roughness Reynolds number R_h with boundary-layer thickness, for the Hartree and the Schlichting velocity profiles.

NACA-Langley - 8-5-53 - 1000